PROCEEDINGS OF SCIENCE

Using gravitational waves to detect axion miniclusters and axion stars

Juan Urrutia[a,b]

[a] *Keemilise ja Bioloogilise Füüsika Instituut, Rävala pst. 10, 10143 Tallinn, Estonia*

[b] *Department of Cybernetics, Tallinn University of Technology, Akadeemia tee 21, 12618 Tallinn, Estonia*

E-mail: juan.urrutia@kbfi.ee

We proposed using GW lensing around axion stars and axion miniclusters as a new avenue to test Axion Dark Matter. Although the prospects are challenging, it is an exciting new test that deserves detailed study to prepare for the new proposed GW detectors.

First Cosmic Whispers Training School
Sep 11-14, 2023
Rettorato Universita' del Salento, Lecce, Italy

PoS(COSMICWISPers)046

This short overview is based on the talk given at the First Cosmic Whispers Training School by the author, which was based on the original work [3], all the plots showcased here are taken from there.

Lensing of gravitational waves by axion stars and axion miniclusters

Imagine a binary system emitting gravitational waves (GWs) at the angular diameter distance D_s. As these waves travel toward the detector, they encounter a Dark Matter (DM) structure at the angular diameter distance D_l. This DM structure influences the curvature of spacetime, leading to gravitational lensing of the signal. We will consider the lensing by a DM axion star inside an axion minicluster. In the frequency domain, the gravitational wave signal, affected by gravitational lensing, is represented as $\tilde{\phi}_L(f) = F(f)\tilde{\phi}(f)$, where $\tilde{\phi}(f)$ is the original signal, and $F(f)$ denotes the amplification factor. This amplification factor, which essentially is an integral over all paths that the GW can take around the DM star, can be expressed as [6]

$$F(w, \boldsymbol{y}) = \frac{w}{2i\pi} \int \mathrm{d}^2\boldsymbol{x}\, e^{iwT(\boldsymbol{x},\boldsymbol{y})}\,, \tag{1}$$

where the integral is taken over the lens plane. Utilizing a system's characteristic length scale, denoted as ξ_0, the dimensionless vectors $\boldsymbol{x}$ and $\boldsymbol{y}$, which are vectors in the lens plane, are defined as $\boldsymbol{x} \equiv \boldsymbol{\xi}/\xi_0$ and $\boldsymbol{y} \equiv D_l\boldsymbol{\eta}/(D_s\xi_0)$, where $\boldsymbol{\eta}$ is the vector denoting the position of the source in the source plane and $\boldsymbol{\xi}$ denotes the position in the lens plane. Physically $\boldsymbol{y}$ can be interpreted as the the adimensional projection of the source in the lens plane and $\boldsymbol{x}$ the position at which the GW crosses the lens plane. Additionally, the dimensionless frequency w and the dimensionless time delay function T are expressed as follows:

$$w \equiv \frac{(1+z_l)D_s}{D_l D_{ls}}\xi_0^2 2\pi f\,, \qquad T(\boldsymbol{x},\boldsymbol{y}) \equiv \frac{1}{2}|\boldsymbol{x}-\boldsymbol{y}|^2 - \psi(\boldsymbol{x}) - \phi(\boldsymbol{y})\,. \tag{2}$$

Here, f is the GW signal frequency, and $D_{ls} = D_s - D_l(1+z_l)/(1+z_s)$ stands for the angular diameter distance between the lens and the source, $\psi(x)$ is the lens potential and encodes all the information concerning the mass distribution in the lens plane. We refer to $y \equiv |\boldsymbol{y}|$ as the impact parameter. The function $\phi(\boldsymbol{y})$ is defined so that the minimum of $T(\boldsymbol{x},\boldsymbol{y})$ with respect to $\boldsymbol{x}$ is zero, expressed as $\min_{\boldsymbol{x}} T(\boldsymbol{x},\boldsymbol{y}) = 0$.

We will consider the case that there are axion miniclusters with axion stars inside them which are soliton solutions of the axion field. If the GW wavelength is proportional to the size of the axion minicluster, then the main interaction effect is going to come from the star which we approximated as a uniform sphere profile. It is characterized by its mass M_l and radius R. The mass density of the lens is defined as follows

$$\rho(r) = \frac{3M_l}{4\pi R^3}\,\theta(R-r)\,. \tag{3}$$

Choosing ξ_0 to be the Einstein radius ($\mathrm{R_E}$) of the axion minicluster as if it was a point mass and defining $b \equiv R/\xi_0$, we find that the deflection potential for a uniform density sphere is

$$\psi(x) = \begin{cases} \frac{1}{3}\sqrt{1-\frac{x^2}{b^2}}\left(\frac{x^2}{b^2}-4\right) + \ln\left(b+\sqrt{b^2-x^2}\right)\,, & x \le b\,, \\ \ln x\,, & x > b\,. \end{cases} \tag{4}$$

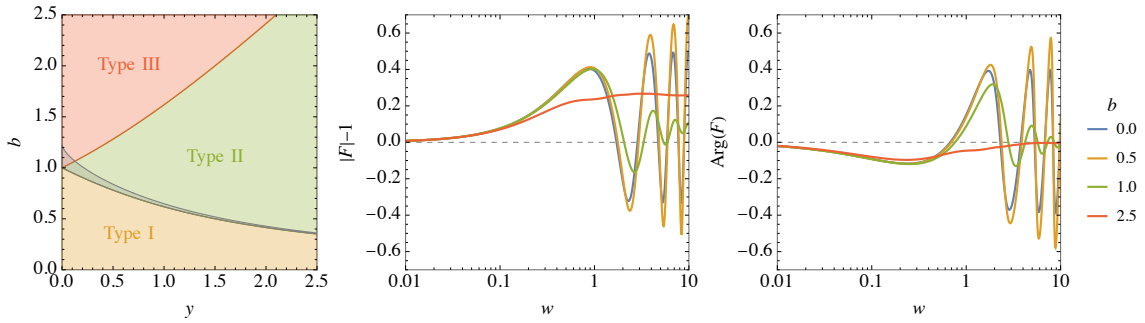

Figure 1: The left panel illustrates the regions corresponding to the three types of lensing by the Axion star, as discussed in the main text. In the middle and right panels, the modulus and argument of the amplification function F are presented as functions of the dimensionless frequency w for various lens sizes b, with $y = 1$ held constant. In this context, the $b = 0$ case corresponds to the point mass lens, $b = 0.5$ is denoted as type I, $b = 1$ as type II, and $b = 2.5$ as type III lensing, as showed in the left panel.

There are two classical paths around the axion star that the GW can take, meaning those that solve the classical equations of motion. This produces three distinctive regimes of lensing, if both paths lay inside the R_E of the lens we call it Type I, if only the minimum time path is inside it we call it Type II and if no path is inside it we call it Type III. In Fig.1 we show the three types of interactions and what region in the b, y plane corresponds to each of the regimes.

Suppose, on the other hand, that the GW wavelength is much longer than the axion star and comparable to the axion minicluster size. In that case, the axion minicluster is going to be the main profile interacting with the GW. We approximate the axion minicluster profile by the Navarro–Frenk–White (NFW) density profile, which is described by the scale radius r_s

$$\rho(r) = \frac{r_s^3 \rho_s}{r\,(r_s + r)^2}\,, \tag{5}$$

and has a deflection potential

$$\psi(x) = \kappa \left[\ln^2\!\left(\frac{x}{2b}\right) - \operatorname{artanh}^2 \sqrt{1 - \frac{x^2}{b_2^2}} \right]. \tag{6}$$

Here, we introduce dimensionless parameters, $\kappa \equiv 2\pi\rho_s r_s^3/M_{\rm v}$, where $M_{\rm v}$ is the virial mass, and $b_2 \equiv r_s/\xi_0$. The distances are also normalized by $\xi_0 = R_E(M_v)$, and with this specific choice of ξ_0, the dimensionless frequency is expressed as $w = 8\pi(1+z_l)M_{\rm v} f$. The modulus and argument of the amplification function are depicted for various halo viral masses in Fig. 2. When $M_{\rm v} < 10^{10} M_\odot$, we observe that $\kappa \lesssim 0.3$ and $b > 2$. For these specific values of κ and b, only one path extremizes the time delay T, crossing the lens plane at approximately $\boldsymbol{x} \approx \boldsymbol{y}$. As illustrated in Fig. 2, the amplification function resembles the Type III case for a uniform-density sphere lens.

After comprehending the interaction with GWs, it becomes essential to determine the probability of encountering a sufficiently lensed GW such as it is detectable. The probability of detecting a lensed GW, assuming a Poisson distribution, is expressed as

$$P_l = 1 - e^{-\tau}\,, \tag{7}$$

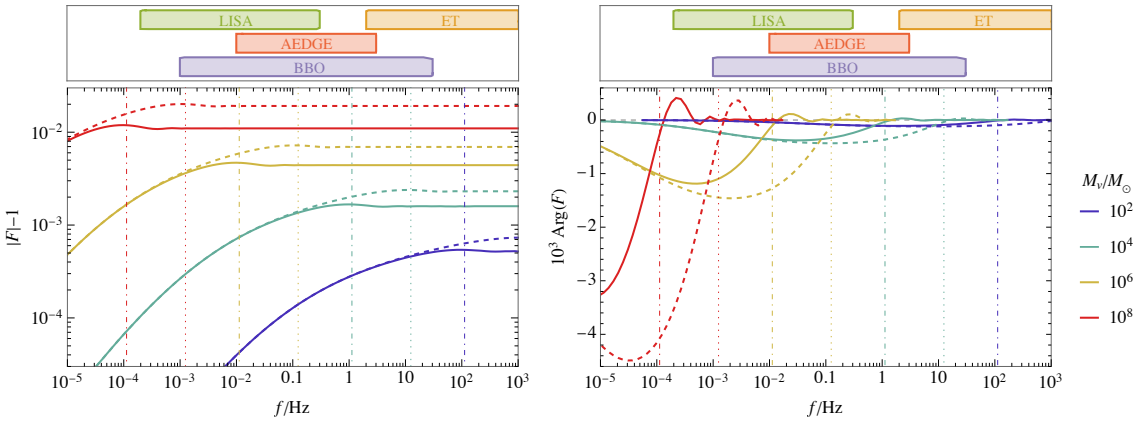

Figure 2: The magnitude and phase of the amplification function F are depicted for an NFW halo lens across varying frequencies, considering different virial masses of the halo. Solid and dashed curves represent scenarios with $y = 1$ and $y = 0.3$, respectively, while keeping the source and lens luminosity distances fixed at $D_{\rm sL} = 5$,Gpc and $D_{\rm lL} = 2.5$,Gpc. Vertical lines mark the location of the maximum of $|F|$, and the frequency ranges pertinent to different experiments are also highlighted.

where τ represents the optical depth linked to the lensing cross-section. The optical depth is defined as

$$\tau(z_s) = \int_0^{D_s} \mathrm{d}V\, n(D_l)\frac{\sigma(D_l)}{4\pi D_l^2} = \int_0^{z_s} \mathrm{d}z_l \frac{n(z_l)\sigma(z_l)}{(1+z_l)H(z_l)}\,, \tag{8}$$

here $\mathrm{d}V = 4\pi D_l^2 \mathrm{d}D_l$ represents the differential volume element. The variables n and H denote the number density of the lenses and the Hubble expansion rate, respectively. The cross-section for detecting the lens effect in a given GW signal is given by

$$\sigma = \pi\xi_{\rm max}^2 = \pi\xi_0^2 y_{\rm max}^2\,, \tag{9}$$

where $\xi_{\rm max} = \xi_0 y_{\rm max}$ represents the maximum impact parameter of the source-lens-detector system, beyond which the detectability of the lens effect is below some fixed statistical certainty which we considered to be at the 2σ CL.

Detectable event prospects

For light axion masses, the halo mass function can exhibit notable deviations from the Cold Dark Matter (CDM) case. Firstly, the suppression of small-scale fluctuations leads to a low-mass cutoff in the halo mass function at approximately $M_v \sim (m_a/10^{-15}\mathrm{eV})^{-3/2} M_\odot$ (refer to, e.g., [5]). Secondly, beyond the structures formed post-matter-radiation equality, some miniclusters may have formed before matter-radiation equality [4]. Utilizing findings from Ref. [2], we observe that the present-day DM halos generated from these miniclusters introduce a peak in the halo mass function at $M_v \simeq 5\times 10^5 (m_a/10^{-15}\mathrm{eV})^{-3/2} M_\odot$ (more than 5 orders of magnitude above the cutoff mass).

Moreover, the axion miniclusters are expected to host an axion star. The axion star mass $M_{\rm c}$ can have a range of values for a given minicluster virial mass $M_{\rm v}$. We assess the variability in core masses by leveraging the findings from Ref. [1]. We assume that the distribution of core masses is

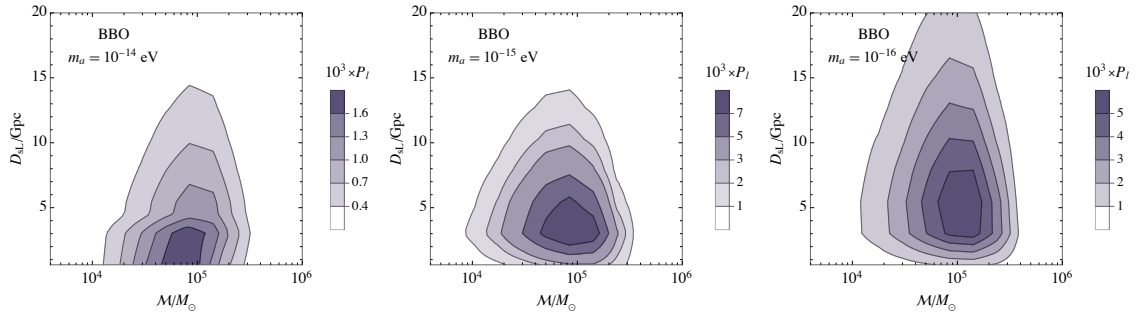

Figure 3: Probability of lensing by a DM halo or axion minicluster for three axion masses.

uniform in logarithmic scale within the range $M_{c,1} < M_c < M_{c,2}$ as provided by the fitting formula

$$\frac{M_{c,j}}{M_\odot} = \beta_j \left(\frac{m_a}{10^{-17}\text{eV}}\right)^{-3/2} + \gamma_j \left(\frac{m_a}{10^{-17}\text{eV}}\right)^{3(\alpha_j-1)/2} \left(\frac{M_v}{10^6 M_\odot}\right)^{\alpha_j}, \tag{10}$$

with $\alpha_1 = 0.33$, $\beta_1 = 0.062$ and $\gamma_1 = 26$, and $\alpha_2 = 0.64$, $\beta_2 = 0.19$ and $\gamma_2 = 2.1 \times 10^3$.

For low-frequency GWs, coming for example from intermediate-mass Black Holes mergers, the main effect of the lensing is going to come from the minihalos DM profile as we do not expect so heavy axion star. We focus on displaying BBO results since they are the most optimistic. In Fig. 3, we present the lensing probability for BBO, considering a halo mass function that incorporates both CDM halos and the additional bump originating from miniclusters, we do it for three different axion masses, denoted by m_a.

For higher-frequency GWs, we focus in the LIGO and ET frequency ranges, which are more sensitive to the axion stars. In Fig. 4 we showcase the probability of detecting these cores for $m_a = 10^{-17}$ eV, considering both LIGO and ET. This particular axion mass results in the highest microlensing probability, as a lighter axion mass renders the cores non-compact and a heavier axion mass quickly brings the lensing into a regime where the interference condition is violated and no interference between paths occurs making the lensing of GWs more difficult to detect.

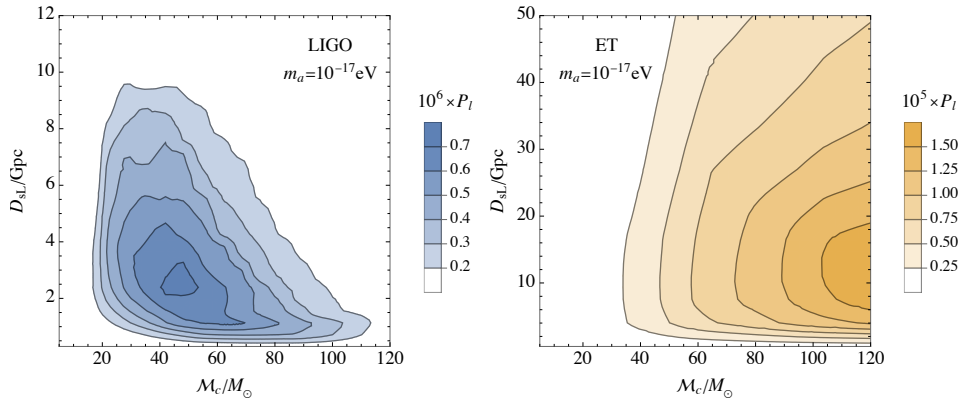

Figure 4: The likelihood of detecting lensing caused by fuzzy dark matter cores is presented as a function of source parameters, considering $m_a = 10^{-17}$ eV.

Acknowledgments

The author is thankful to the organizers of the First Cosmic Whispers Schools as well as to Ville Vaskonen for valuable comments. This article is based on work from COST Action COSMIC WISPers CA21106, supported by COST (European Cooperation in Science and Technology). This work was supported by the Estonian Research Council grants PRG803, PSG869, RVTT3 and RVTT7 and the Center of Excellence program TK202.

References

[1] Hei Yin Jowett Chan, Elisa G. M. Ferreira, Simon May, Kohei Hayashi, and Masashi Chiba. The diversity of core–halo structure in the fuzzy dark matter model. *Mon. Not. Roy. Astron. Soc.*, 511(1):943–952, 2022.

[2] Malcolm Fairbairn, David J. E. Marsh, Jérémie Quevillon, and Simon Rozier. Structure formation and microlensing with axion miniclusters. *Phys. Rev. D*, 97(8):083502, 2018.

[3] Malcolm Fairbairn, Juan Urrutia, and Ville Vaskonen. Microlensing of gravitational waves by dark matter structures. *JCAP*, 07:007, 2023.

[4] Edward W. Kolb and Igor I. Tkachev. Axion miniclusters and Bose stars. *Phys. Rev. Lett.*, 71:3051–3054, 1993.

[5] Mihir Kulkarni and Jeremiah P. Ostriker. What is the halo mass function in a fuzzy dark matter cosmology? *Mon. Not. Roy. Astron. Soc.*, 510(1):1425–1430, 2021.

[6] P. Schneider, J. Ehlers, and E.E. Falco. *Gravitational Lenses*. Astronomy and Astrophysics Library. Springer New York, 2012.